Dalton Transactions

ROYAL SOCIETY OF CHEMISTRY

PAPER

View Article Online
View Journal | View Issue

Cite this: *Dalton Trans.*, 2025, **54**, 12913

Coordination and C–H activation of an amidobis(phosphaalkene) ligand at rhodium(I)†

Kushik,[a] Mirko Rippke,[a] Hans-Joachim Drexler,[a] Fabian Dankert,[b] Christian Hering-Junghans *[a] and Torsten Beweries *[a]

Received 23rd July 2025,
Accepted 23rd July 2025

DOI: 10.1039/d5dt01734c

rsc.li/dalton

Phosphaalkenes are an underrepresented class of phosphorus-based ligands that hold great potential for the stabilisation of low-valent transition metal and main group fragments. We present the synthesis of a monoanionic PNP-type bis-phosphaalkene ligand and its reactions with $[Rh(cod)(Cl)]_2$, which furnish two unique dinuclear Rh(I) complexes. These complexes show C–H activation of the Mes* groups of the PNP ligand and the presence of three different phosphaalkene coordination modes, respectively. Computational analyses suggest the presence of a unique Rh–Rh donor–acceptor interaction in the C–H-activated complex. Stabilisation of the desired tricoordinate PNP-supported Rh(I) species is possible in the presence of the strongly donating CO ligand, yielding a mononuclear square-planar complex of the type [(PNP)Rh(CO)].

Introduction

Phosphaalkenes (PAs), $RP{=}CR_2$, are organophosphorus compounds characterised by a P=C double bond and are related to alkenes and imines as their lighter group 15 homologues,[1] showing great potential for various applications in modern organophosphorus chemistry.[2] The coordination chemistry of PAs to transition metals is characterised by their unique ligand properties (HOMO P=C π-bond, high s character of the lone pair at P, and inverse polarity of the $P^{(\delta+)}$–$C^{(\delta-)}$ bond), making these compounds weaker σ-donors than imines, but considerable π-acceptors due to the low-lying P–C π* orbital (LUMO). Coordination of neutral PA ligands to late transition metals has been reported on several occasions,[3] and some of such complexes have found applications in stoichiometric and catalytic transformations such as N–H activation,[4] aza-Claisen rearrangements,[5] or upgrading of alcohols.[6]

Although tri-[7] and tetradentate[8] PNP- (Fig. 1, top left) and PPPP-type PAs have been reported, to the best of our knowledge, mono-anionic PNP pincer-type PA architectures have not been designed to date. The coordination chemistry of tridentate ligands is well-studied for related amido-bis(phosphines), and their structural variety and versatility for synthesis and catalysis has been highlighted on several occasions.[9] Recent examples include work by Ozerov and co-workers on phosphine-based group 9 PNP systems bearing diphenylamine based amido-bis(phosphine) ligands (Fig. 1, top right) for alkyne dimerisation and C–H activation,[10] as well as studies by Gade and co-workers on the stabilisation of unusual T-shaped 14-electron Rh(I) using amido-bis(phosphine) PNP ligands based on a carbazole backbone.[11] In the latter case, Rh(I) is κ^3-coordinated by the PNP ligand with additional stabilisation

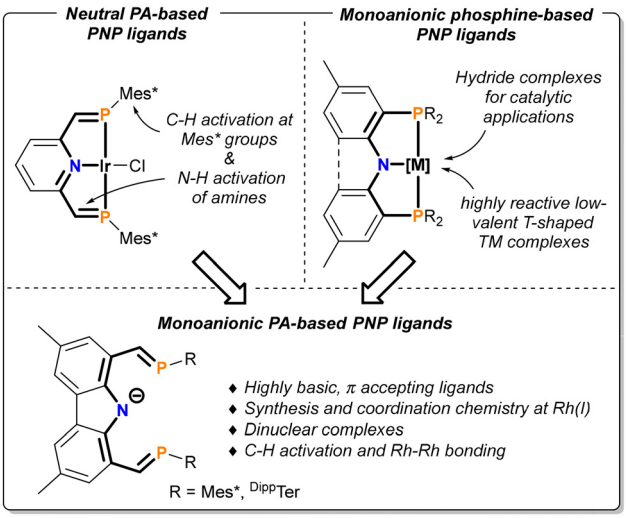

Fig. 1 Contextualisation of this work. Mes* = 2,4,6-tBu_3-C_6H_2, ^{Dipp}Ter = 2,6-(2,6-$iPr_2C_6H_3$)-C_6H_3.

[a]*Leibniz-Institut für Katalyse e.V. (LIKAT Rostock), Albert-Einstein-Str. 29a, 18059 Rostock, Germany. E-mail: Christian.hering-junghans@catalysis.de, Torsten.beweries@catalysis.de*

[b]*University of Kassel, Heinrich-Plett Str. 40, 34132 Kassel, Germany*

†Electronic supplementary information (ESI) available: Synthesis and characterization of compounds, NMR spectra, and crystallographic and computational details. CCDC 2451040–2451044 and 2474838. For ESI and crystallographic data in CIF or other electronic format see DOI: https://doi.org/10.1039/d5dt01734c

enabled through non-covalent interactions with flanking P*t*Bu$_2$ groups.

An extension of the concept of electronically unique PA ligands to tridentate, monoanionic representatives is desirable, since the resulting pincer ligands would create a well-defined reactive site due to their meridional coordination to the metal in combination with the sterically demanding flanking substituents that are typically required for the stabilisation of PAs (Fig. 1, bottom). The resulting monoanionic system should possess the typical electronic properties of PAs and at the same time be able to stabilise highly reactive low-valent transition metals, such as Fe(I) complexes,[12] potentially without the need for additional stabilising L-type ligands at the metal centre. In this contribution, we present the synthesis and characterisation of the first monoanionic bis-PA ligands along with their coordination chemistry to Rh(I), resulting in the formation of two dinuclear Rh complexes that possess intact as well as C–H-activated PA donor sites, as well as a rare Rh(I)–Rh(I) donor–acceptor interaction in one case.

Results and discussion

Novel PNP-based bis-PA pincer ligands were synthesised by treating 3,6-dimethyl-9*H*-carbazole-1,8-dicarbaldehyde (**A**) with two equivalents of the phospha-Wittig reagent Mes*PPMe$_3$ (Mes* = 2,4,6-*t*Bu$_3$-C$_6$H$_2$)[13] in benzene at 50 °C for 24 hours in the absence of light, giving the desired bis-PA ^{Mes*2}PNP (**1a**, Scheme 1) in good yield.

^{31}P{^{1}H} NMR analysis shows the PA units at 249.9 ppm, at the lower end of literature reported Mes*-substituted PA ligands (δ(^{31}P) 250 to 291 ppm),[3] presumably due to delocalisation of electron density from the carbazole unit to the P–C π* orbitals. When heating a mixture of ^{Dipp}TerPPMe$_3$ and **A** in benzene in a 2 : 1 ratio at 80 °C for 14 days, the analogous PNP ligand ^{DippTer2}PNP with ^{Dipp}Ter groups on the P atoms (**1b**) was prepared (Scheme 1, see the ESI† for details). The ^{31}P{^{1}H} NMR spectrum of the reaction mixture showed the characteristic resonance for the bis-PA PNP ligand **1b** at 239.5 ppm. In addition, the mono-PA PNO species **1b′**, with only one PA arm and an intact aldehyde group,[14] is formed as indicated by a resonance at 244.6 ppm. In the ^{1}H NMR spectrum of **1b′**, three deshielded resonances for the NH (10.80 ppm), C(O)H (9.73 ppm) and P=CH (9.23 ppm) protons, with the NH only showing a doublet signature, underline the presence of a single PA arm. In contrast, the bis-PA PNP ligands **1a** and **1b** show a triplet resonance (11.29 ppm, C$_6$D$_6$, J_{PH} = 11.6 Hz) for the NH proton due to coupling with two P atoms. The formation of **1b′** can be suppressed, though, when using a slight molar excess of ^{Dipp}TerPPMe$_3$. This facilitates selective access of **1b**.

Crystals of **1a** suitable for single-crystal X-ray diffraction (SC-XRD) analysis were obtained from a saturated *n*-hexane solution at −30 °C overnight. SC-XRD analysis of **1a** (Fig. 2) revealed the expected structure of the ^{Mes*2}PNP ligand with moderate hydrogen-bonding interactions between the N–H proton and both phosphorus atoms of the PA units, resulting in *E*-configured PA units (P1–C15 1.679(2) Å, P2–C34 1.686(2) Å), with both Mes* substituents pointing away from the binding pocket. In **1b**, both PA units are likewise *E*-configured (Fig. S2†), while one of the P atoms points away from the carbazole N atom to account for the increased steric strain from the ^{Dipp}Ter substituents. In both **1a** and **1b**, the P=C bonds are nearly co-planar with the carbazole backbone.

To facilitate transmetalation, ligand **1a** was deprotonated using the non-nucleophilic bases M[N(SiMe$_3$)$_2$] (M = Na, K), in either benzene or THF at room temperature, yielding the alkali metal complexes [Na(^{Mes*2}PNP)] (**2a**) and [K(^{Mes*2}PNP)] (**3a**) in quantitative yields as red or violet solids, respectively. According to TD-DFT calculations, the red colour of **2a** is associated with a π–π* transition, with the Na$^+$ resulting in a smaller HOMO–LUMO gap compared to **1a** and thus a red shift in the longest wavelength absorption ($\lambda_{max,calc}$(**2a**) = 546.3 nm). Both salts are highly moisture sensitive, necessitating careful handling under strictly anhydrous conditions. The deprotonation of **1a** was confirmed by ^{1}H NMR spectroscopy, revealing the absence of the deshielded N–H signal. Moreover, IR spectroscopy showed the absence of the N–H stretching mode in the spectra of **2a** and **3a** (**1a**: $\tilde{\nu}$(N–H) = 3300 cm^{-1}). The ^{31}P{^{1}H} NMR spectra of the salts show considerably shielded signals for the Na salt **2a** (δ(^{31}P) = 228.4 ppm) and the K salt **3a** (δ(^{31}P) = 236.8 ppm) compared to the free ligand **1a**,

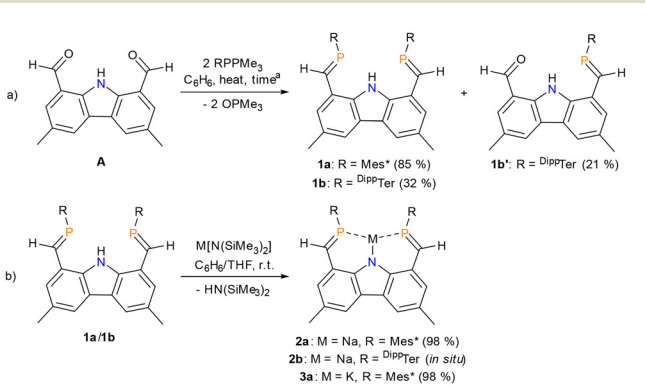

Scheme 1 (a) Synthesis of novel ^{R2}PNP PA ligands **1a** and **1b**. [a] Conditions for **1a**: C$_6$H$_6$, 50 °C, 24 h; for **1b**: C$_6$H$_6$, 80 °C, 14 d. (b) Synthesis of M[^{Mes*2}PNP] (M = Na (**2a**) and K (**3a**)).

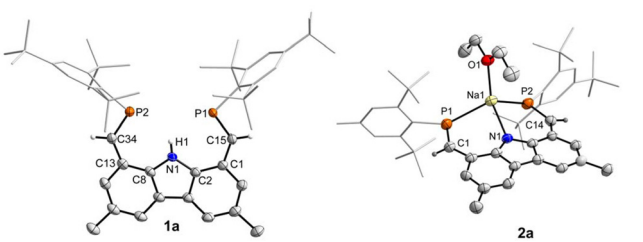

Fig. 2 Molecular structures of **1a** (left) and **2a** (right). ORTEP diagrams are drawn at 50% probability. H atoms (except NH and RP = CHR) are omitted, and Mes* groups are rendered as wireframes for clarity.

reflecting the subtle electronic differences induced by the counterions. SC-XRD-quality red crystals of **2a** were afforded by slow diffusion of Et_2O into a saturated *n*-hexane solution of **2a** at room temperature. The molecular structure of **2a** shows the sodium ion in a distorted seesaw coordination environment ($\tau_4 = 0.32$)[15] with the fourth coordination site occupied by Et_2O (note that Et_2O is only present in the solid state), resulting in Na located above the PNP mean plane. The sodium contacts to the PNP ligand are in the expected range for elongated Na–N (Na1–N1 2.324(3) Å; Σr_{cov}(Na–N) = 2.26 Å)[16] and Na–P single bonds (Na1–P1 2.735(2) Å, Na1–P2 2.732(2) Å; Σr_{cov}(Na–P) = 2.66 Å).[16] The PA units coordinate to Na in κ^P-fashion through the s-type lone pair on P, as indicated by short P–C distances (P1–C1 1.674(4) Å, P2–C14 1.673(4) Å).

Next, **2a** was reacted with $[Rh(cod)(Cl)]_2$ in THF in a 2 : 1 molar ratio (Scheme 2), accompanied by a colour change from red to dark brown. The $^{31}P\{^1H\}$ NMR spectrum of the reaction mixture revealed two species, free ligand **1a** ($\delta(^{31}P)$ = 249.9 ppm) and a second species giving a doublet at 46.7 ppm ($^1J_{P-Rh}$ = 132 Hz), indicative of a Rh(I) complex (Scheme 2). The significant shielding of the ^{31}P NMR signal compared to ligand **1a** and two sets of doublets with a large $^2J_{H-H}$ coupling of 14 Hz for four diastereotopic benzylic protons in the ^1H NMR spectrum indicated that the Mes*P = CH unit underwent intramolecular C–H addition/cyclisation to form a phospholanylmethyl (phosphaindane) moiety.[17] Such cyclisation reactions have been reported for PN-type PAs (*e.g.*, $[Rh(quin\text{-}P,N)_2]$OTf, $\delta(^{31}P)$ = 55.1 ppm)[3a,b] and BPEP-based systems [RhCl(Mes*$_2$-BPEP), $\delta(^{31}P)$ = 28.9 ppm].[18]

Surprisingly, SC-XRD analysis of green crystals obtained from a concentrated THF solution layered with *n*-pentane and stored at ambient temperature revealed the formation of the dinuclear Rh(I) phosphaindane complex **4** (Fig. 3, left). The formation of such dinuclear species can be rationalised by the intermediate formation of a T-shaped 14 electron complex, which then undergoes C–H bond activation of the *o*-*t*Bu groups and eventually adds a second equivalent of [Rh(cod)Cl]. When not considering the Rh–Rh interaction (Rh1–Rh2 2.6334(9) Å, *cf.* Σr_{cov}(Rh–Rh) = 2.50 Å), Rh2 resides in a trigonal pyramidal coordination sphere, coordinated by cod and the carbazole N atom. This rather unusual coordination sphere for a 16-valence electron complex makes the metal centre Lewis-acidic.[19,20] In contrast, Rh1 is best described as a 16-valence

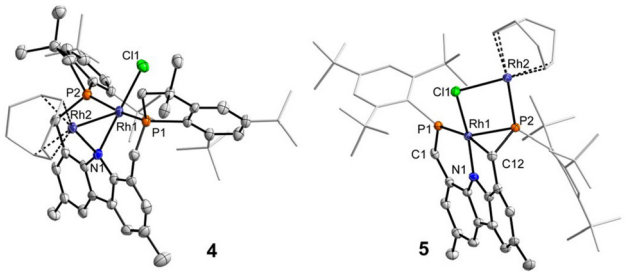

Fig. 3 Molecular structures of complexes **4** and **5**. ORTEP diagrams are drawn at 50% probability. For clarity, hydrogen atoms are omitted, and Mes* groups and cod ligands are rendered as wireframes for clarity.

electron square-planar Rh(I) centre (not considering the Rh–Rh interaction), making the metal centre Lewis-basic. Rh1 is coordinated by both phosphaindane arms in a *trans*-arrangement (Rh1–P1 2.311(2) Å, Rh1–P2 2.317(2) Å), in addition to Cl^- and the carbazole N atom. Both metal centres are bridged by the carbazole N atom, with inequivalent Rh2–N1 (2.094(6) Å) and Rh1–N1 (2.149(7) Å) distances.

To elucidate the Rh–Rh bonding in complex **4**, DFT studies at the PBE0-D3/def2-SVP level of theory were carried out (see the ESI† for details). The HOMO is best described as non-bonding with significant d-orbital contributions at both Rh centres with a higher coefficient at the square-planar Rh1 centre. The Rh1–Rh2 interaction is represented in HOMO−1 (Fig. 4, top left) and shows donation from a d_{z^2} on Rh1 to a d-orbital at Rh2, while the Rh–N bonding is represented in HOMO−2 and HOMO−5. The LUMO is metal centred, and thus the longest wavelength absorption ($\lambda_{max,exp.}$ = 652 nm, $\lambda_{max,calc.}$ = 609 nm) can be best described as a metal-to-metal charge transfer (HOMO–LUMO transition). An NBO analysis also shows a d_{z^2} orbital on Rh1 (Fig. 4, top right), which is delocalised into a d-type lone valence at Rh2. In the NBO

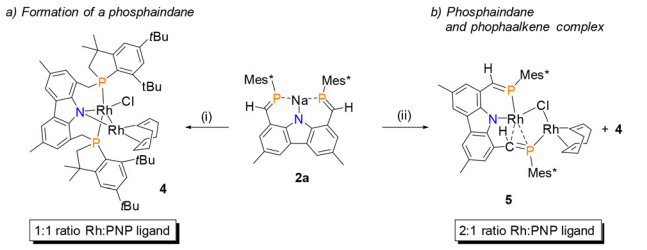

Scheme 2 Reactions of **2a** with varying amounts of $[Rh(cod)(Cl)]_2$. Conditions: (i) 0.5 $[Rh(cod)(Cl)]_2$, THF, 1 h, r.t.; (ii) $[Rh(cod)(Cl)]_2$, THF, 1 h, r.t.

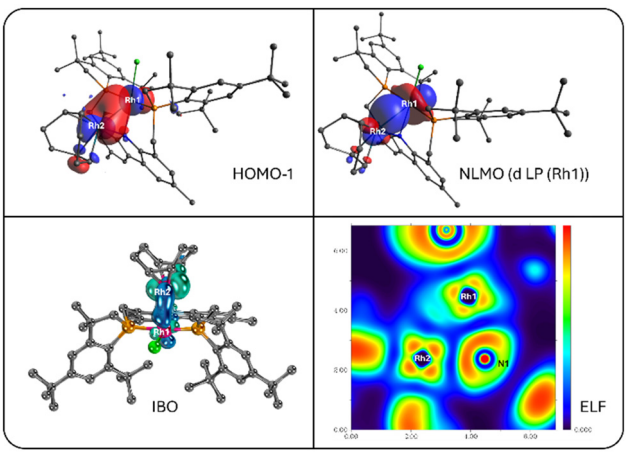

Fig. 4 Illustration of the Rh–Rh interaction in complex **4**. HOMO−1 (PBE0-D3/def2-SVP), NLMO of a d_{z^2} type lone pair (LP) on Rh1, IBO of the Rh–Rh interaction (r2SCAN-3c//PBE0-D3/def2-SVP), and electron localisation function (ELF, PBE0-D3/def2-SVP).

picture, the sp^2-type lone pair on the carbazole N atom is delocalised into d-type lone valencies at each Rh centre. Complementary IBOs also illustrate the donor–acceptor character of the Rh–Rh bond (Fig. 4, bottom left, Fig. S86), while the electron localisation function (ELF) shows considerable localised electron density between the Rh atoms (Fig. 4, bottom right). In line with this, AIM analyses show a bond critical point.

Next, the reaction of **2a** and $[Rh(cod)(Cl)]_2$ in a 1 : 1 molar ratio was studied to explore whether full ligand consumption could be achieved. The reaction mixture in THF at room temperature revealed the formation of **4** according to $^{31}P\{^1H\}$ NMR spectroscopy, along with a new set of signals: a doublet at 169.2 ppm ($^1J_{P-Rh}$ = 152 Hz) and a doublet of doublets at 125 ppm ($^1J_{P-Rh}$ = 157 Hz, $^1J_{P-Rh}$ = 70 Hz). These lower field signals suggest the presence of intact P=C units and of another dinuclear Rh(I) species. SC-XRD analysis of dark red crystals revealed the first example of a dinuclear Rh(I) complex featuring three different coordination modes of its PA units (Fig. 3, right). Both Rh atoms are μ-bridged by a chloride, and one of the PA units (P2–C12 1.765(3) Å) shows both a side-on η^2-coordination to Rh1 and end-on η^1–κ^P coordination to Rh2. The P2–C12 distance is in line with a previously reported η^2-PA Ni complex (*e.g.*, 1.773(8) Å).[21] Even though such a coordination mode has been theoretically considered,[1] this is the first synthetic realisation of PA η^1,η^2-coordination. Interestingly, the P2–C12 PA is *Z*-configured, resulting in π–π interactions of the Mes* group at P2 with the phenyl ring of the carbazole moiety (distance between centroids of both rings = 3.686 Å). The other PA unit shows a considerably shorter P1–C1 bond (1.694(2) Å), in line with P1 coordinating to Rh1 in η^1-fashion. The coordination sphere at Rh1 is saturated by the carbazole N atom (Rh1–N1 1.975(2) Å) in the *trans*-position to the μ-bridging Cl^-. According to TD-DFT studies, the longest wavelength absorption ($\lambda_{max,exp.}$ = 796 nm, $\lambda_{max,calc.}$ = 735 nm) in the UV-Vis spectrum is associated with a HOMO–LUMO transition that can be best described as charge redistribution within the PNP framework with little contribution from the Rh centres. The second absorption at 564 nm is associated with an MLCT process (HOMO−1 to LUMO). The side-on coordination of the P2–C12 arm is best visualised in HOMO−1 and HOMO−5, while in the NBO picture, this interaction is reflected in a Rh–P bonding orbital which is best described as an interaction of a Rh-centred d-orbital with the P–C π* orbital. The discovery of complex **5** adds a novel dimension to the coordination chemistry of PAs, expanding the known modes of interaction with transition metals.

Mechanistically, the formation of complexes **4** and **5** is assumed to be facilitated by a putative, tricoordinate Rh(I) $14e^-$ species. Such complexes have only recently been structurally authenticated and are shown to be highly reactive.[11] This prompted us to test whether starting from $[Rh(Cl)(CO)_2]_2$ the mononuclear $16e^-$ complex of the type LRh(CO) could be isolated, postulating that the small CO ligand could effectively stabilise such a complex. Gratifyingly, when **2a** was combined with $[Rh(Cl)(CO)_2]_2$, irrespective of whether a 1 : 1 or 2 : 1 metal-to-ligand ratio was used, in THF at room temperature, the colour of the reaction mixture turned brown. According to ^{31}P NMR spectroscopy, a new species with a doublet at 181.7 ppm ($^1J_{Rh-P}$ = 163.6 Hz), significantly shielded compared to **2a** and the neutral bis-PA **1**, was detected. The ^1H NMR spectrum indicated a C_{2v} symmetric species in solution, and the complex could be crystallised from the reaction mixture by adding *n*-pentane. SC-XRD experiments confirmed the formation of $[Rh(CO)(^{Mes*2}PNP)]$ (**6**) as a C_{2v} symmetric complex, crystallising in the monoclinic space group *C*2/*c* with eight molecules in the unit cell (Fig. 5). In line with the ^{31}P NMR shift, the P=CH distances (P1–C15 1.666(2) Å; P2–C16 1.663(2) Å) indicate intact PA units, and the sum of angles at Rh (Σ(<Rh) = 360°) is in line with a minimally distorted square-planar geometry. The Rh–CO distance (C53–O1 1.139(3) Å) is in the range of those of related PNP-Rh(I) complexes (*cf.* $[Rh(CO)\{N(CH_2CH_2PCy_2)_2\}]$ 1.1575(14) Å).[22] IR spectroscopy revealed a CO stretching vibration at 1996 cm^{-1}, which is considerably blue-shifted compared to related amido-PNP Rh carbonyl complexes (*cf.* $[Rh(CO)\{N(CH_2CH_2PCy_2)_2\}]$, $\tilde{\nu}$(C≡O) = 1905 cm^{-1}).[22] The UV-vis spectrum shows a longest wavelength absorption at 505 nm, which, according to TD-DFT calculations, corresponds to a π–π* transition ($\lambda_{max,calc}$(**2a**) = 459 nm), in line with orange-coloured crystals. The formation of **6** clearly shows the potential of ligand **1a** to form mononuclear Rh(I) complexes.

To determine whether the observed formation of dinuclear rhodium complexes is exclusive to $[Rh(cod)(Cl)]_2$, further investigations were carried out using related group 9 metal precursors. $^{31}P\{^1H\}$ NMR monitoring of the reactions of **2a** and 1 or 0.5 equivalents of $[Ir(cod)(Cl)]_2$ in THF indicated the formation of the protonated ligand **1a** (250.0 ppm) as the major species along with several unidentified products that show resonances between 20–25 ppm and 150–250 ppm (see the ESI† for details), suggesting unselective formation of PA and phosphaindane complexes. The formation of the protonated form of the ligand, likely through proton abstraction from the solvent, supports the strong basicity of **2a**. While the $^{31}P\{^1H\}$ NMR spectra of the reaction of **2a** with 1 equiv. of $[Rh(coe)_2Cl]_2$ (coe = cyclooctene) show mainly phosphaindane-type signals at *ca.* 50 ppm, when using 0.5 equiv. of $[Rh(coe)_2Cl]_2$ mainly ligand **1a** was obtained. Similarly, reactions

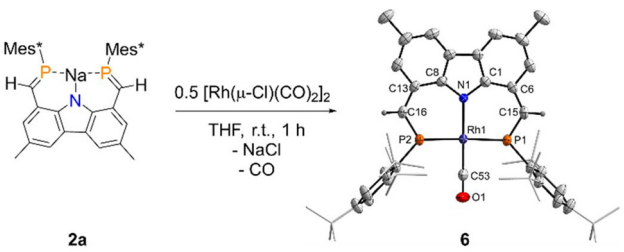

Fig. 5 Reaction of **2a** with $[Rh(Cl)(CO)_2]_2$ giving complex **6**. Molecular structure of complex **6**. ORTEP diagrams are drawn at 50% probability. For clarity, hydrogen atoms (except H15 and H16) are omitted, and *t*Bu-groups are rendered as wireframes for clarity.

of **2a** with $[Rh(nbd)Cl]_2$ (nbd = 2,5-norbornadiene) produce mixtures of several species. However, in this case, the reaction with 1 equiv. of $[Rh(nbd)Cl]_2$ shows minor signals at 172.8 and 137.3 ppm that could correspond to a species similar to **5**. These results suggest that the reactivity leading to **4** and **5** is unique for $[Rh(cod)Cl]_2$ and warrants further exploration to fully understand the underlying mechanisms.

Conclusions

A new class of anionic PNP-type bis-PA ligands **1a** and **1b** based on a carbazole backbone have been prepared, and their facile deprotonation yields the corresponding Na and K salts. With $[Rh(cod)(Cl)]_2$, a unique dinuclear Rh complex with a Rh–Rh donor–acceptor interaction is obtained, while with an excess of the Rh precursor, a bis-PA complex with three different PA-coordination modes was accessed. The formation of such dinuclear complexes suggests the intermediate formation of a T-shaped $14e^-$ electron complex. Such species can be trapped in the presence of the small, strongly donating CO ligand, yielding the square-planar $16e^-$ electron complex **6**. The formation of this species clearly shows the potential of ligand **1a** in organometallic chemistry. Future studies will focus on expanding these concepts to main group elements and to utilise the Rh complexes in catalysis.

Author contributions

K. K.: investigation, data curation, formal analysis, funding acquisition, and writing – original draft. M. R.: investigation and formal analysis. H.-J. D.: investigation and formal analysis. F. D.: DFT calculations. C. H.-J.: conceptualisation, resources, DFT calculations, supervision, and writing – review and editing. T. B.: conceptualisation, funding acquisition, resources, supervision, and writing – review and editing.

Conflicts of interest

There are no conflicts to declare.

Data availability

The data supporting this article have been included as part of the ESI.† Crystallographic data have been deposited at the CCDC under the identification numbers 2451040 (**1a**) 2451041 (**1b**), 2451042 (**2a**), 2451043 (**4**), and 2451044 (**5**), respectively. Further details can be obtained from the authors.

Acknowledgements

We thank the ITMZ at the University of Rostock for access to the cluster computer, and especially Malte Willert for his assistance with the queuing system and software installations. Dr Jonas Bresien (University of Rostock) is acknowledged for providing the SLURM interface for Gaussian. The DFG (HE 7348/3-1) and the Studienstiftung des Deutschen Volkes (U12AB123456) are gratefully acknowledged for financial support. F.D. gratefully acknowledges the Fonds der chemischen Industrie (FCI) for funding through the Liebig-Fellowship scheme.

References

1 P. Le Floch, *Coord. Chem. Rev.*, 2006, **250**, 627–681.
2 A. Ziółkowska, J. Doroszuk and Ł. Ponikiewski, *Organometallics*, 2023, **42**, 505–537.
3 Selected examples: (*a*) P. Gupta, T. Taeufer, J.-E. Siewert, F. Reiß, H.-J. Drexler, J. Pospech, T. Beweries and C. Hering-Junghans, *Inorg. Chem.*, 2022, **61**, 11639–11650; (*b*) M. L. Nakashige, J. I. P. Loristo, L. S. Wong, J. R. Gurr, T. J. O'Donnell, W. Y. Yoshida, A. L. Rheingold, R. P. Hughes and M. F. Cain, *Organometallics*, 2019, **38**, 3338–3348; (*c*) K. W. Magnuson, S. M. Oshiro, J. R. Gurr, W. Y. Yoshida, M. Gembicky, A. L. Rheingold, R. P. Hughes and M. F. Cain, *Organometallics*, 2016, **35**, 855–859; (*d*) Y. Nakajima, Y. Nakao, S. Sakaki, Y. Tamada, T. Ono and F. Ozawa, *J. Am. Chem. Soc.*, 2010, **132**, 9934–9936.
4 Y.-H. Chang, Y. Nakajima, H. Tanaka, K. Yoshizawa and F. Ozawa, *J. Am. Chem. Soc.*, 2013, **135**, 11791–11794.
5 J. Dugal-Tessier, G. R. Dake and D. P. Gates, *Organometallics*, 2007, **26**, 6481–6486.
6 P. Gupta, H. J. Drexler, R. Wingad, D. Wass, E. Barath, T. Beweries and C. Hering-Junghans, *Inorg. Chem. Front.*, 2023, **10**, 2285–2293.
7 A. Jouaiti, M. Geoffroy and G. Bernardinelli, *Tetrahedron Lett.*, 1992, **33**, 5071–5074.
8 P. M. Miura-Akagi, M. L. Nakashige, C. K. Maile, S. M. Oshiro, J. R. Gurr, W. Y. Yoshida, A. T. Royappa, C. E. Krause, A. L. Rheingold, R. P. Hughes and M. F. Cain, *Organometallics*, 2016, **35**, 2224–2231.
9 J. C. Ott, D. Bürgy, H. Guan and L. H. Gade, *Acc. Chem. Res.*, 2022, **55**, 857–868.
10 W. Weng, C. Guo, R. Çelenligil-Çetin, B. M. Foxman and O. V. Ozerov, *Chem. Commun.*, 2006, 197–199.
11 L. K. Paschai Darian, J. Ballmann and L. H. Gade, *Angew. Chem., Int. Ed.*, 2024, **63**, e202416814.
12 Y. Nakajima, Y. Nakao, S. Sakaki, Y. Tamada, T. Ono and F. Ozawa, *J. Am. Chem. Soc.*, 2010, **132**, 9934–9936.
13 P. Gupta, J.-E. Siewert, T. Wellnitz, M. Fischer, W. Baumann, T. Beweries and C. Hering-Junghans, *Dalton Trans.*, 2021, **50**, 1838–1844.
14 K. Kushik, A. Petrov, D. Ranieri, L. Edelmann, T. Beweries and C. Hering-Junghans, *Angew. Chem., Int. Ed.*, 2024, **63**, e202412982.
15 L. Yang, D. R. Powell and R. P. Houser, *Dalton Trans.*, 2007, 955–964.

16 P. Pyykkö and M. Atsumi, *Chem. – Eur. J.*, 2009, **15**, 12770–12779.
17 F. Ozawa and Y. Nakajima, *Chem. Rec.*, 2016, **16**, 2314–2323.
18 H.-o. Taguchi, Y.-H. Chang, K. Takeuchi and F. Ozawa, *Organometallics*, 2015, **34**, 1589–1596.
19 D. Ostendorf, C. Landis and H. Grützmacher, *Angew. Chem., Int. Ed.*, 2006, **45**, 5169.
20 C. Schweinzer, P. Coburger and H. Grützmacher, *Adv. Sci.*, 2024, **11**, 2400072.
21 A. H. Cowley, R. A. Jones, C. A. Stewart, A. L. Stuart, J. L. Atwood, W. E. Hunter and H. M. Zhang, *J. Am. Chem. Soc.*, 1983, **105**, 3737–3738.
22 R. Jaeger, S. G. Rachor, M. Ahrens and T. Braun, *Chem. – Eur. J.*, 2024, **30**, e202401571.